Surface coating with $Ca(OH)_2$ for improvement of the transport of nanoscale zero-valent iron (nZVI) in porous media

Cai-jie Wei and Xiao-yan Li*

Environmental Engineering Research Centre, Department of Civil Engineering, The University of Hong Kong, Pokfulam, Hong Kong.
(E-mail: *cjwei@hku.hk; xlia@hkucc.hku.hk*)

Abstract
A novel thermal deposition method was developed to coat $Ca(OH)_2$ on the surface of nanoscale zero-valent iron (nZVI). The nZVI particles with the $Ca(OH)_2$ coating layer, nZVI/$Ca(OH)_2$, had a clear core-shell structure based on the TEM observations, and the $Ca(OH)_2$ shell was identified as an amorphous phase. The $Ca(OH)_2$ coating shell would not only function as an effective protection layer for nZVI but also improve the mobility of nZVI in porous media for its use in environmental decontamination. A 10% Ca/Fe mass ratio was found to result in an proper thickness of the $Ca(OH)_2$ shell on the nZVI surface. Based on the filtration tests in sand columns, the $Ca(OH)_2$-based surface coating could greatly improve the mobility and transport of nZVI particles in porous media. In addition, batch experiments were conducted to evaluate the reactivity of $Ca(OH)_2$-coated nZVI particles for the reduction of Cr(VI) and its removal from water.

Keywords: Zero-valent iron (ZVI); nano-core/shell structure; calcium hydroxide ($Ca(OH)_2$); transportation in porous media

INTRODUCTION

Zero valent iron (ZVI) has demonstrated its great reactivity and potential for *in-situ* groundwater and soil remediation (Li *et al*. 2006; Yan *et al*. 2013). Its high capability of dechlorination and effective immobilization of heavy metals have been well documented (Kanel *et al*. 2005; Lv *et al*. 2011). For field applications, ZVI can be used from micrometers to nanometers in size with different levels of reactivity and efficiency for decontamination. The high reducing activity of nanoscale ZVI (nZVI) for environmental decontamination has been recognized in recent years. nZVI may be injected with water to the pollution sites for *in-situ* remediation, which can be much more flexible and cost-effective compared to installation of conventional ZVI materials (e.g. reactive ZVI barriers). However, nZVI reacts readily with non-targeted substances such as dissolved oxygen and water during application. Such side reaction results in rapid formation of passive ferric iron (Fe(III)) oxides, leading to a complete loss of nZVI's reducing capacity (Sarathy *et al*. 2008). Thus, it is essential to maintain the reactivity of nZVI before its designated environmental applications. Moreover, research shows that particle-particle interaction (aggregation) and particle-grain interaction (deposition) limit the transport and delivery of nZVI particles in porous media (Phenrat et al., 2009). The ferric oxide shell on the nZVI surface also has a strong affinity to sand grains (Saleh *et al*., 2007). The aggregation and deposition of nZVI would greatly reduce its mobility in the saturated subsurface environment.

Effort has been made to improve the stability and mobility of nZVI for its effective environmental application. Different types of chemical stabilizers and surfactants, such as polyacrylic acid,

carboxymethycellulose, starch and humic matter, were used to ensure the dispersion of nZVI in suspension (He and Zhao 2005; Kanel and Choi 2007; Sun *et al*. 2007). By entrapment of nZVI particles into the silica matrix, iron/silica composites were synthesized to prevent the particle aggregation while maintaining the iron reactivity (Zhan *et al*. 2008). Oil in water emulsion was substantiated to be effective for good delivery of iron nanoparticles in porous media (Mueller *et al*. 2012). These methods may either enhance the dispersion or increase the corrosion resistance of nZVI particles in the environment; however, none of the methods is able to achieve these two purposes simultaneously. Moreover, the surface modification reagents are either too expensive for large scale engineering applications or potential pollutants to the subsurface environment.

The purpose of the study was to coat a protective shell on nZVI to improve its stability and mobility. The core-shell structure synthesis refers to the technology that coats appropriate shell materials onto the surface of the target particles. If the shell materials can be well formed on the nZVI surface, the shell would protect nZVI particles from both corrosion and aggregation. For surface coating on particles, moderately soluble inorganic salts may be considered as the shell materials. In fact, there are already reports of metal salt particles, such as $CaCO_3$ and $Ca(OH)_2$, formed at the nanoscale (Salvadori *et al*. 2001; Li *et al*. 2002; Niemann *et al*. 2006; Alavi *et al*. 2010; Liu *et al*. 2010). Such materials can form a dense structure to protect ZVI particles, and they are also more economic and environmentally safe than surfactants and other polymeric substances. In this study, a new method has been developed that is to coat a $Ca(OH)_2$ layer on the nZVI surface to protect it from oxidation while greatly improve its mobility and transport in porous media. For potential environmental applications, the reactivity of $Ca(OH)_2$-coated nZVI particles for the reduction and immobilization of Cr(VI) was also evaluated.

MATERIALS AND METHODS

Materials – nZVI particles

Nano-sized zero valent iron (nZVI) was a commercial product purchased from Nabond Technologies Co., China (http://www.nabond.com). According to microscopic observations, the size of single nZVI particles was around 40 nm. However, owing to magnetic clustering, the particles had a mean size of around 500 nm, as determined by a laser diffraction particle size analyzer (LS13 320 Beckman Coulter). While, nZVI had a density of about 7.5 g/cm^3, the coating layer of $Ca(OH)_2$ had a density of 2.21 g/cm^3.

Coating of $Ca(OH)_2$ on nZVI particles

The thermal deposition method was employed to form a $Ca(OH)_2$ coating shell onto nZVI particles. While nZVI particles were suspended in a NaOH solution (0.25M) in methanol, a methanol solution of $CaCl_2$ (0.125M) was quickly injected into the solution. Polyacrylic acid (PAA) was added as a dispersing agent for nZVI, and the particle suspension was placed in a sonication bath at 60 ^oC during the coating process. Owing to the low solubility of $Ca(OH)_2$ at an elevated temperature, $Ca(OH)_2$ would precipitate on the surface of nZVI particles. After a predetermined coating period or time, nZVI particles were washed thorough with ethanol to remove residual ions in solution, and nZVI was magnetically separated from $Ca(OH)_2$ particles. The nZVI with $Ca(OH)_2$ coating, or nZVI/Ca, was then ground by ball milling in ethanol, and the particles were dried and stored with N_2 protection before experimental use.

Characterization of the $Ca(OH)_2$ shell

The Ca content coated on nZVI was determined by an inductively coupled plasma (ICP) spectrometry (PerkinElmer, OptimaTM8000) after acid digestion of the nZVI/Ca powder. The size

distribution of nZVI particles was measured by the particle size analyzer (Beckman Coulter). The crystal forms of the coating materials on nZVI were analyzed by an X-ray diffraction (XRD) (Bruker AXS D8) system. For XRD detection, the particle powder had been pressed into a test pellet about 0.5 mm in thickness. The nZVI/Ca particles were characterized for the morphology and core-shell structure by a transmission electron microscopy (TEM) (Philips Tecnai G2 20 S-TWIN), together with the technique of energy-dispersive X-ray spectroscopy (EDS) for the elemental distribution profile of the samples.

Filtration experiments

Filtration tests were conducted to evaluate the mobility and transport of the commercial nZVI particles in porous media. A 10 cm filter column 1.1 cm in internal diameter (total volume = 9.50 mL) was packed with either clean silica sand (d_{50} = 732 μm) or spherical glass beads (GB) (d_{50} = 901 μm) as the model porous material. The pore volume was 3.77 mL in the sand column and 3.64 mL in the glass column. The nZVI particle concentration in the feed solution was 1 g/L with a $CaCl_2$-$Ca(OH)_2$ buffer at pH~7.5. The nZVI suspensions were pumped through the filters at an empty-bed filtration velocity of 1.83 m/hr. The nZVI concentrations in the feed (C_0) and filtrate (C) were determined from the measurement of the iron contents in the water samples by an atomic absorption (AA) spectroscopy (PerkinElmer, AAnalyst 300).The Ca content after its dissolution in water was also measured by the AA.

Batch tests on Cr(VI) reduction and immobilization by nZVI particles

Nano-size ZVI particles were synthesized for the tests on their reactivity for the reduction and immobilization of hexavalent chromium (Cr(VI)). nZVI was produced in the laboratory following the method of borohydride reduction of ferric chloride ($FeCl_3 \cdot 6H_2O$), which is a primary and effective method for the synthesis of iron nanoparticle (Wang *et al*., 2009). The Cr(III) removal experiments were conducted on three types of nZVI particles for comparison, including bare nZVI, nZVI/Ca-2h, and nZVI/Ca-2h after the $Ca(OH)_2$ shell being washed off by water. For a test, nZVI particles were placed in a 40-mL glass vial filled with the Cr(VI) solution. The vial was completely sealed by a screw cap and placed on a rotary shaker (MMV14, Heto-Holten) at 25 ^oC and 150 rpm. The initial Cr concentration was 20 mg/L and the nZVI content was 2.5 g/L. During the Cr(VI) reduction test, 1 mL of the suspension was withdrawn at different time intervals from the test vial using a syringe under N_2 protection. The sample was then filtered by a 0.45 μm nylon membrane (Millipore), and the Cr concentration in the filtrate was measured by the ICP spectrometry (PerkinElmer, OptimaTM8000) that has a detection limit for total Cr as low as 5 μg/L. From the change of the Cr concentration in water, the rate of CI(VI) reduction and immobilization by the nZVI particles was determined.

RESULTS AND DISCUSSION

With the thermal deposition, $Ca(OH)_2$ was coated on the nZVI surface. The coating duration was tested from 1 to 2 h, and the amount of Ca coated was about 7% of the nZVI weight after 1 h coating, which increased to 10% after 2 h coating (Fig. 1). The number weighted average hydrodynamic radius increased from 861.6 nm for the bare nZVI (B-nZVI) to 1123.6 nm for the coated nZVI after 1 hr coating (nZVI/Ca-1h) and further to 1459.4 nm for the nZVI after 2 h coating (nZVI/Ca-2h) (Fig. 2). The particle size increase was consistent with the coating $Ca(OH)_2$ content, suggesting a shell layer formation on the nZVI particles.

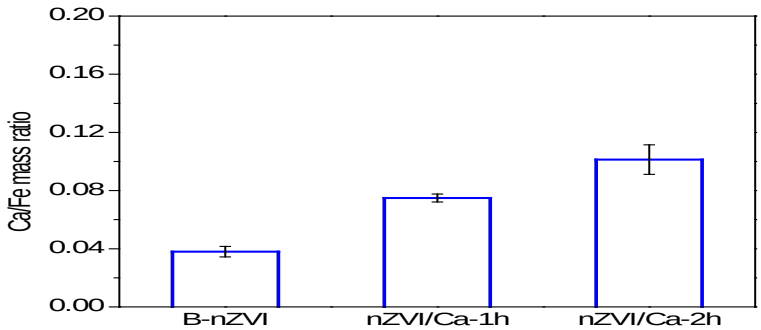

Fig. 1. The content of $Ca(OH)_2$ coated on the nZVI particles under different coating conditions.

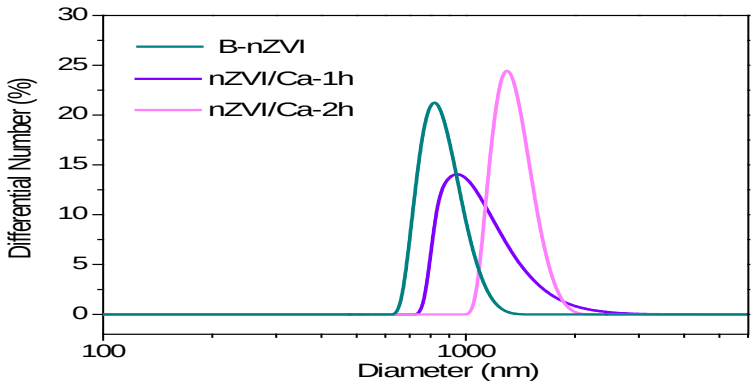

Fig. 2. Size distributions of the bare nZVI and $Ca(OH_{)2}$-coated nZVI particles.

For the nZVI after 2 h of coating, the Ca/Fe ratio was around 0.1. The TEM images show that single nZVI particle had a diameter of about 50 nm. Thus, it can be estimated that there was an average thickness of about 5 nm for the $Ca(OH)_2$ shell on the nZVI surface based on the Ca/Fe ratio. The shell formation on nZVI particles can be observed from the TEM images (Fig. 3). Based on the EDS elemental mapping result (Fig. 4), a Ca-based shell (yellow) can be further identified around the Fe core (green). The Ca shell layer is around 5-10 nm in thickness according to the TEM mapping image, which is consistent with the estimation of thickness from the Ca content.

The chemical forms of $Ca(OH)_2$ coated on nZVI were further characterized by the XRD (Fig. 5). No obvious XRD peaks of $Ca(OH)_2$ crystals were found for the $Ca(OH)_2$ coating layer, whilst pure $Ca(OH)_2$ particles formed without the presence of nZVI appeared to be crystals. The comparison between the XRD profiles suggest that $Ca(OH)_2$ deposited on the nZVI surface was in the amorphous phase that can be readily dissolved in water.

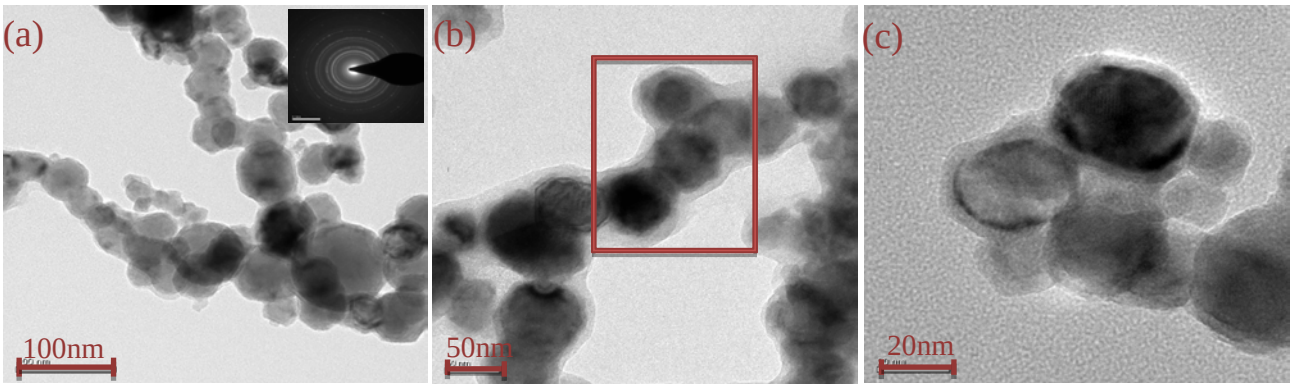

Fig. 3. TEM images of (a) bare nZVI, (b) and (c) nZVI/Ca particles.

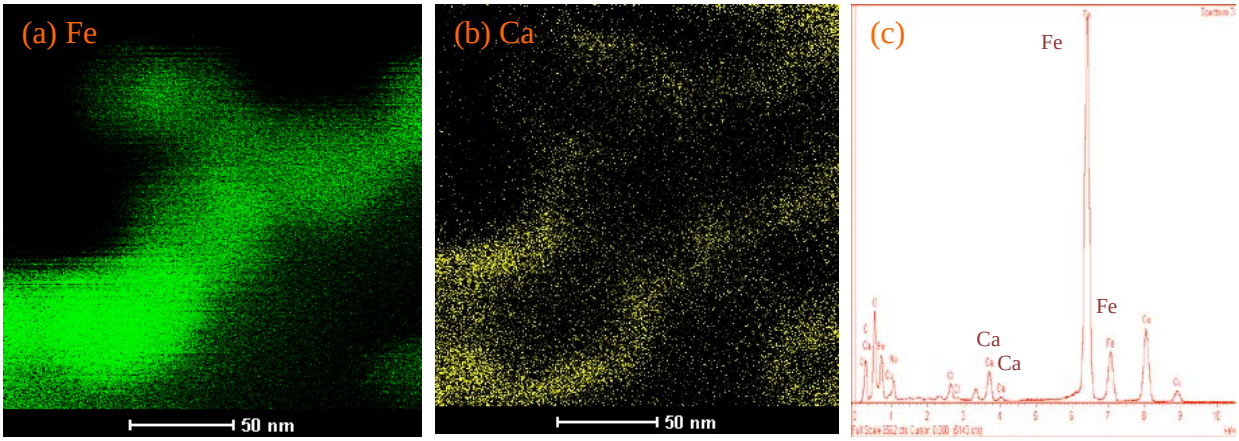

Fig. 4. (a) & (b) EDS elemental mapping result for nZVI/Ca-2h particles (for the TEM scope in the red box in Fig. 3c), and (c) the corresponding EDS spectrum.

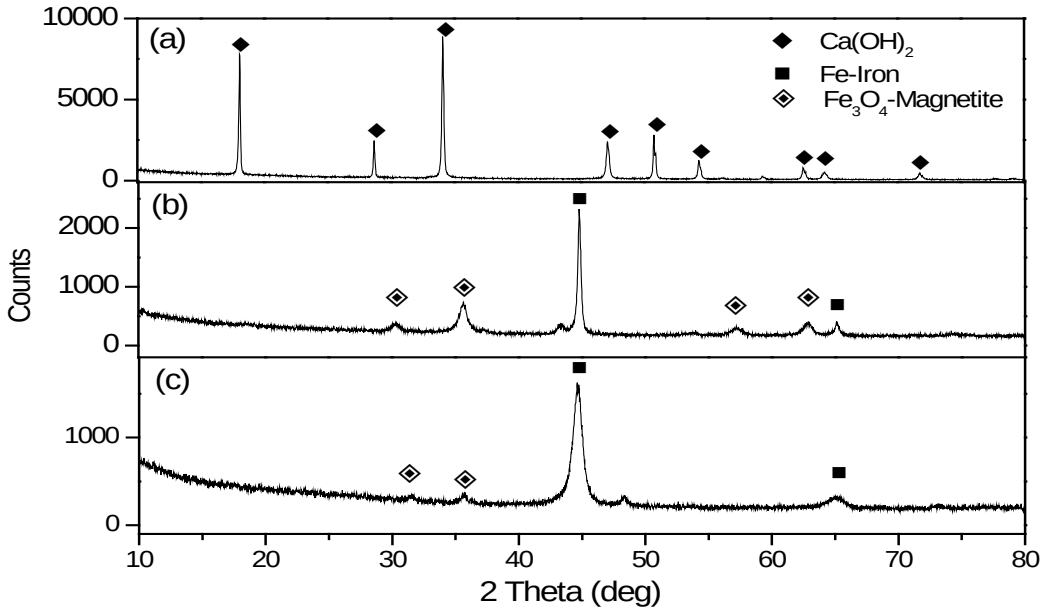

Fig. 5. XRD spectra of (a) pure $Ca(OH)_2$ powders formed in methanol, (b) $Ca(OH)_2$ coated on the nZVI particles and (c) bare-nZVI .

Transport of nZVI/$Ca(OH)_2$ particles in filter columns

Filtration of nZVI particles with water through the sand and glass columns demonstrate the mobility and transport behavior of the particles in porous media. The penetration of nZVI particles during filtration in the filter columns can be well observed in Fig. 6. For the bare-nZVI without $Ca(OH)_2$ coating, the particles deposited mostly on the top of filters in both the sand and glass columns. There was no passage of iron particles in the effluent after 60 min of filtration. In comparison, for the $Ca(OH)_2$-coated nZVI, particles penetrated through filter media rather rapidly, and the dark iron particles could fill up the entire filter columns in a few minutes. Breakthrough of nZVI/Ca particles appeared in the effluent after only 3 or 4 pore volumes of water filtration.

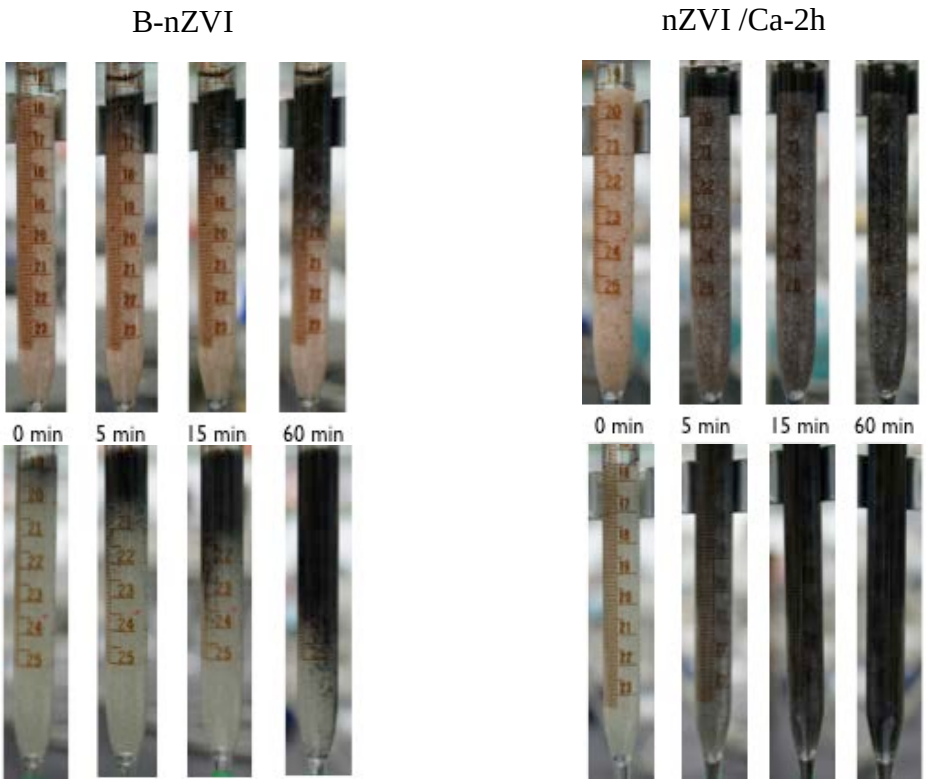

Fig. 6. Filtration of bare nZVI particles (left) and $Ca(OH)_2$ coated nZVI particles (right) through filter columns. (Top row: sand column; bottom row: GB column)

The breakage curves of B-nZVI and nZVI/Ca particles are presented in Fig. 6. Bare-nZVI had a low mobility and could not penetrate through the filter media. All of B-nZVI particles were trapped in the filter columns, keeping the C/C_0 ratio at the zero level. With the surface $Ca(OH)_2$ coating, around 60% or more of nZVI particles could pass through the sand filters. In the GB filters, the C/C_0 ratio could achieve 50% for nZVI/Ca-1h and 60% for nZVI/Ca-2h. The results show that coating of $Ca(OH)_2$ on the nZVI surface can significantly improve the mobility and transport of nZVI particles in porous media.

The breakthrough data in Fig. 7 can be further used to analyze the attachment efficiency and transport behavior of different nZVI particles in the filter media, based on the following filtration equations (Yao *et al*. 1971):

$$\ln\frac{C}{C_0} = -\frac{3}{2}(1-f)\alpha\eta_0\left(\frac{L}{d_c}\right)$$

where C and C_0 are the particle concentrations in the influent and effluent, respectively, and the C/C_0 ratio can be obtained from the breakthrough curve, d_c is the diameter of single spherical collector, α is the particle attachment efficiency, f is the porosity of the filter column, L is the filter length, η_0 is the predicted clean bed single-collector efficiency. The η_0 value for given particles through a porous medium filter can be determined using the filtration model of Tufenkji and Elimelech (2004).

Based on the η_0 values and C/C_0 results, the attachment efficiency (α) and the transport distances of different nZVI particles in porous media can be determined (Table 1). With the $Ca(OH)_2$ coating, the attachment potential of nZVI particles greatly decreased, implying a much improved mobility.

Accordingly, the transport distance of the particles with 1% penetration content ($L_{1\%}$) or 0.1% penetration content ($L_{0.1\%}$) increased significantly in both filter media. Compared to bare nZVI, the $L_{0.1\%}$ distance for nZVI-Ca particles increased by more than 10 times from 0.10 to 1.11 m in the sand column and from 0.12 to 1.36 m in the GB column.

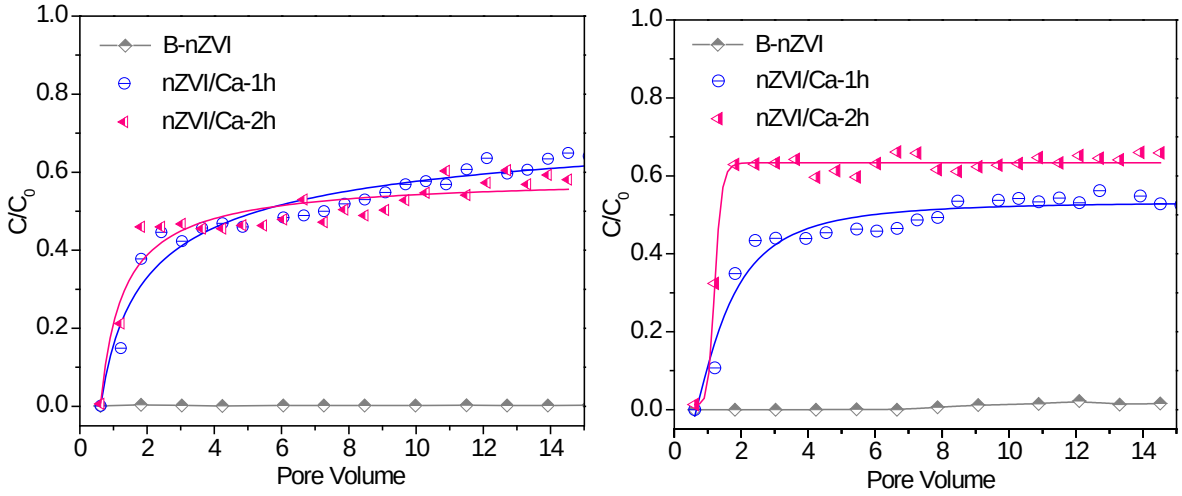

Fig. 7. Filtration and breakthrough curves of bare nZVI and $Ca(OH)_2$-coated nZVI particles in sand (left) and GB (right) columns.

Based on the η_0 values and C/C_0 results, the attachment efficiency (α) and the transport distances of different nZVI particles in porous media can be determined (Table 1). With the $Ca(OH)_2$ coating, the attachment potential of nZVI particles greatly decreased, implying a much improved mobility. Accordingly, the transport distance of the particles with 1% penetration content ($L_{1\%}$) or 0.1% penetration content ($L_{0.1\%}$) increased significantly in both filter media. Compared to bare nZVI, the $L_{0.1\%}$ distance for nZVI-Ca particles increased by more than 10 times from 0.10 to 1.11 m in the sand column and from 0.12 to 1.36 m in the GB column.

Table 1. The filtration parameters (α, $L_{1\%}$ and $L_{0.1\%}$) of nZVI particles in the sand and GB column.

	C/C_0	α	$L_{1\%}$	$L_{0.1\%}$
B-nZVI_sand	0.002	7.73	0.10	0.15
nZVI/Ca-1h_sand	0.587	0.735	1.15	1.73
nZVI/Ca-2h_sand	0.574	0.798	1.11	1.66
B-nZVI_GB	0.013	6.92	0.12	0.18
nZVI/Ca-1h_GB	0.547	1.07	0.87	1.30
nZVI/Ca-2h_GB	0.682	0.705	1.36	2.05

Cr(VI) reduction and immobilization by various types of nZVI particles

The batch experimental results show that nZVI particles were highly reactive for the reduction and removal of hexavalent chromium in water (Fig. 8). With the reduction by nZVI, Cr(IV) could be converted to Cr(III) that readily precipitated as a solid hydroxide on nZVI particles (Li *et al.*, 2008; Shih *et al.*, 2011). The high reduction capability of bare nZVI particles was well demonstrated, which achieved a 90% Cr(VI) removal in less than 30 min. With the $Ca(OH)_2$-coating layer, the reactivity of nZVI for Cr(VI) reduction was somewhat reduced. This could be also contributed to the pH increase (to pH~10.5) from the dissolution of $Ca(OH)_2$ that was supposed to be unfavorable to Cr(VI) reduction (Lv *et al.*, 2011). Nonetheless, the nZVI/Ca particles were still effective to

reduce Cr(VI) and remove Cr from water, with over 85% Cr being removed in 3 hr. More importantly, when the $Ca(OH)_2$ coating layer was washed off (nZVI/Ca-W) before the batch test, the reactivity of nZVI could be fully recovered for Cr(VI) reduction, for which more than 90% Cr could be removed from water in about 20 min (Fig. 8a). The Cr removals by different nZVI types can be well fitted by the pseudo-first order reaction kinetics ($R^2 > 0.9$). The rate constants for Cr(VI) reduction by B-nZVI, nZVI/Ca and nZVI/Ca-W particles are 0.064, 0.013 and 0.072 min^{-1}, respectively (Fig. 8b). The batch test results imply that, while the $Ca(OH)_2$ shell improves the stability and mobility of nZVI particles for potential environmental applications, the coating layer has no apparent effect on the reactivity of nZVI for *in-situ* remediation.

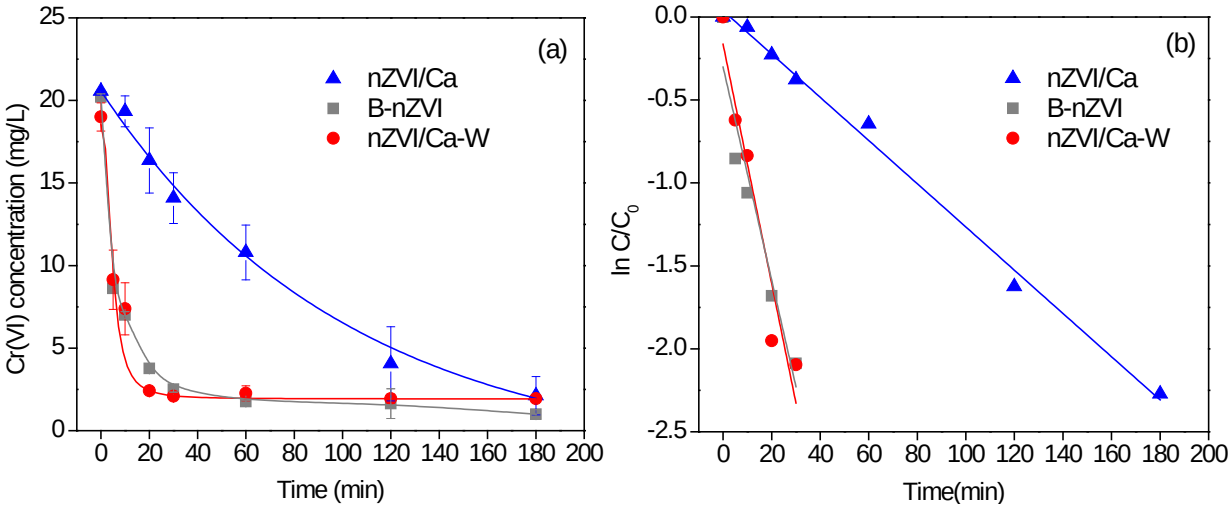

Fig. 8. Reduction and removal of Cr(VI) in water by bare nZVI (B-nZVI), nZVI/Ca-2h (nZVI/Ca) and nZVI/Ca-2h after the $Ca(OH)_2$ coating layer being washed off (nZVI/Ca-W).

CONCLUSIONS

A novel thermal deposition method was developed to coat a $Ca(OH)_2$ shell on the surface of nZVI particles. The $Ca(OH)_2$ coating layer can effectively protect nZVI and greatly improve its transport and delivery in porous media. The batch test results show that, once the $Ca(OH)_2$ shell is dissolved, the reactivity of nZVI for Cr(VI) reduction and immobilization can be fully recovered.

ACKNOWLEDGEMENTS

This research was supported by grants HKU714811E and from the Research Grants Council (RGC) and AoE/P-04/2004 from the University Grants Committee (UGC) of the Hong Kong SAR Government. The technical assistance of Mr. Keith C. H. Wong is greatly appreciated.

REFERENCES

Alavi, M.A. and Morsali, A. (2010). Ultrasonic-assisted synthesis of $Ca(OH)_2$ and CaO nanostructures. *Journal of Experimental Nanoscience*, **5**(2), 93-105.

He, F. and Zhao, D. (2005). Preparation and Characterization of a new class of starch-stabilized bimetallic nanoparticles for degradation of chlorinated hydrocarbons in Water. *Environmental Science & Technology*, **39**(9), 3314-3320.

Kanel, S.R., Manning, B., Charlet, L. and Choi, H. (2005). Removal of Arsenic(III) from Groundwater by Nanoscale Zero-Valent Iron. *Environmental Science & Technology*, **39**, 1291-1298.

Kanel, S.R. and Choi, H. (2007). Transport characteristics of surface-modified nanoscale zero-valent iron in porous media. *Water Science & Technology*, **55**(1-2), 157-164.

Li, M. and Mann, S. (2002). Emergent nanostructures: Water-induced mesoscale transformation of surfactant-stabilized amorphous calcium carbonate nanoparticles in reverse microemulsions. *Advanced Functional Materials,* **12**(11-12), 773-779.

Li, X.Q., Daniel, W.E. and Zhang, W.X. (2006). Zero-valent iron nanoparticles for abatement of environmental pollutants: materials and engineering aspects. *Critical Review of Solid State Material Science*, **31**, 111-122.

Li, X.Q.; Cao, J.S.; Zhang, W.X. (2008). Stoichiometry of Cr(VI) immobilization using nanoscale zerovalent iron (nZVI): A study with high-resolution X-ray photoelectron spectroscopy (HR-XPS). *Industrial & Engineering Chemistry Research*, **47(7)**, 2131-2139.

Liu, T., Zhu, Y.R., Zhang, X.Z., Zhang, T.W., Zhang, T. and Li, X.G. (2010). Synthesis and characterization of calcium hydroxide nanoparticles by hydrogen plasma-metal reaction method. *Materials Letters*, **64**(23), 2575-2577.

Lv, X.S., Xu, J., Jiang, G.M. and Xu, X.H. (2011). Removal of chromium(VI) from wastewater by nanoscale zero-valent iron particles supported on multiwalled carbon nanotubes. *Chemosphere*, **85**, 1204-1209.

Mueller, N.C., Braun, J., Bruns, J., Cernik, M., Rissing, P., Rickerby, D., Nowack, B., (2012). Application of nanoscale zero valent iron (NZVI) for groundwater remediation in Europe. *Environmental Science and Pollution Research,* **19**, 550-558.

Niemann, B., Rauscher, F., Adityawarman, D., Voigt, A. and Sundmacher, K. (2006). Microemulsion-assisted precipitation of particles: Experimental and model-based process analysis. *Chemical Engineering and Processing*, **45**(10), 917-935.

Phenrat, T., Kim, H.-J., Fagerlund, F., Illangasekare, T., Tilton, R.D., Lowry, G.V. (2009). Particle Size Distribution, Concentration, and Magnetic Attraction Affect Transport of Polymer-Modified Fe(0) Nanoparticles in Sand Columns. Environmental Science & Technology, **43**, 5079-5085.

Saleh, N., Sirk, K., Liu, Y., Phenrat, T., Dufour, B., Matyjaszewski, K., Tilton, R.D., Lowry, G.V. (2007). Surface modifications enhance nanoiron transport and NAPL targeting in saturated porous media. *Environmental Engineering Science,* **24,** (1), 45-57.

Salvadori, B. and Dei, L. (2001). Synthesis of $Ca(OH)_2$ nanoparticles from diols. *Langmuir,* **17**, 2371-2374.

Sarathy, V. Tratnyek, P.G. Nurmi, J.T. Baer, D.R. Amonette, J.E. Chun, C.L. Penn, R.L. and Reardon, E.J. (2008). Aging of iron nanoparticles in aqueous solution: Effects on structure and reactivity. *The Journal of Physical Chemistry C*, **112**, 2286–2293.

Shi, L.N., Zhang, X., Chen, Z.L. (2011). Removal of Chromium (VI) from wastewater using bentonite-supported nanoscale zero-valent iron. *Water Research*, **45(2)**, 886-892.

Sun, Y.P., Li, X.Q., Zhang, W.X. and Wang, H.P. (2007) A method for the preparation of stable dispersion of zero-valent iron nanoparticles. *Colloids and Surfaces A: Physicochemical and Engineering Aspects,* **308**(1-3), 60-66.

Tufenkji, N. and Elimelech, M. (2004). Correlation equation for predicting single-collector efficiency in physicochemical filtration in saturated porous media. *Environmental Science & Technology,* **38**, 529-536.

Wang, Q.L., Kanel, S.R., Park, H., Ryu, A. and Choi, H. (2009) Controllable synthesis, characterization and magnetic properties of nanoscale zerovalent iron with specific high Brunauer-Emmett-Teller surface area. *Journal of Nanoparticle Research*, **11**, 749-755.

Yan, W., Lien, H.L., Koel, B.E. and Zhang, W.X. (2013). Iron nanoparticles for environmental clean-up: recent developments and future outlook. *Environmental Science: Processes Impacts*, **15**, 63-77.

Yao, K.-M., Habibian, M.T., O'Melia, C.R. (1971). Water and waste water filtration. Concepts and applications. *Environmental Science & Technology,* **5**, 1105-1112.

Zhan, J., Zheng, T., Piringer, G., Day, C., McPherson, G.L., Lu, Y., Papadopoulos, K. and John, V.T. (2008). Transport characteristics of nanoscale functional zerovalent iron/silica composites for in situ remediation of trichloroethylene. *Environmental Science & Technology*, **42**(23), 8871-8876.